■ Scientific Justification

Section 1

Circumstellar disks of gas and dust are a natural by-product of the star formation process and provide the raw material for planet formation. Hence, their evolution and dispersal determine when and what types of planets can form. *Here, we propose to use MIRI MRS to map the winds from two disks with large dust cavities, constrain the ionization fraction in the flow, and wind mass loss rates. Our observations and analysis will establish how much time is left in these systems to complete planet formation and migration.*

Disk evolution and dispersal timescales. Infrared and millimeter surveys of nearby star-forming regions have established that the typical protoplanetary disk lifetime is a few Myr but the disk dispersal timescale, i.e. the transition from disk-bearing to disk-less, is an order of magnitude shorter (e.g., Ercolano & Pascucci 2017 for a recent review). While the relative roles of viscous accretion vs. magnetohydrodynamic (MHD) disk winds in driving evolution is debated (e.g., Turner et al. 2014), *photoevaporation driven by high-energy stellar photons from the central star* has been long recognized as critical to the dispersal process (Clarke et al. 2001). According to the classic evolutionary picture (e.g., Alexander et al. 2014 and Figure 1), viscous accretion slowly depletes disk material and when the disk accretion rate falls below the photoevaporative wind loss rate, photoevaporation takes over and quickly clears the disk. Thus, photoevaporation effectively ends giant planet formation (e.g. Shu et al. 1993) and limits planet migration which, in turn, impacts the final architecture of planetary systems (e.g., Alexander & Pascucci 2012, Jennings et al. 2018). *Our proposed observations have the potential to provide the first maps of these photoevaporative winds.*

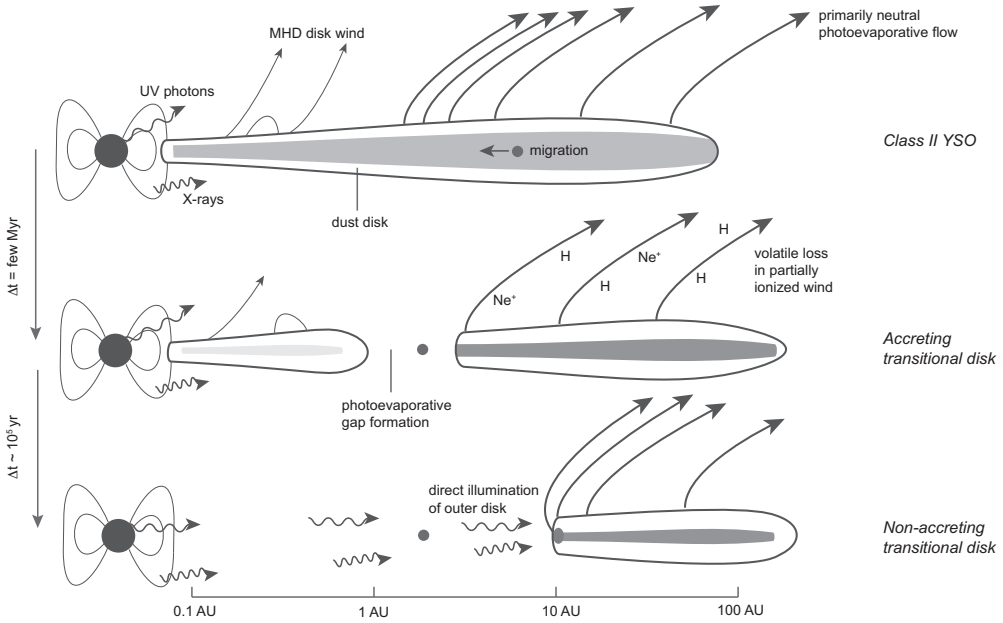

Figure 1: Schematic representation of the classic evolutionary picture of disk evolution and dispersal (Alexander et al. 2014).

Cosmic neon lights the way is the title of the *Spitzer* Science Center press release announcing the discovery of ionized neon towards isolated low-mass stars with disks (Espaillat et al. 2007, Lahuis et al. 2007, Pascucci et a. 2007). These [Ne II] 12.81 μm detections led to

the important realization that Ne^+ might trace a hot ($\geq 1,000$ K) disk atmosphere ionized and heated by high-energy stellar photons (X-rays and/or EUV). Follow-up ground-based high-resolution spectroscopy targeting the brightest infrared disks demonstrated that the [Ne II] 12.81 μm line is a critical diagnostic of disk winds (e.g., Herczeg et al. 2007, Pascucci & Sterizk 2009, Baldovin-Saavedra et al. 2012). Disks with large gaps or dust cavities, hereafter *transitional disks* (see also Figure 1), have single peaked [Ne II] profiles characterized by modest widths (FWHM$\sim$15-40 km/s) and small blueshifts ($\sim$3-6 km/s) in the centroid velocity with respect to the stellar velocity (e.g., Pascucci & Sterizk 2009, Sacco et al. 2012 and Figure 2), consistent with earlier predictions from photoevaporative winds (Alexander 2008). *The blueshifts are a clear tell-tale sign of a slow wind with [Ne II] emission mostly tracing disk radii where dust grains are still present in the midplane*, as dust is the main source of opacity and blocks view of the redshifted outflowing gas (e.g., Ercolano & Owen 2010, Pascucci et al. 2011).

Section 2

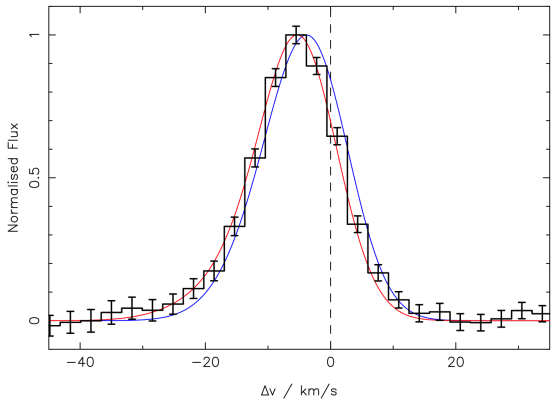

Figure 2: [Ne II] 12.81 μm at $R \sim 30,000$ from the near face-on disk of TW Hya (black line and errorbars, Pascucci et al. 2011). The observed blueshift from the stellar velocity represents an unambiguous detection of a slow, ionized wind. However, these spatially unresolved observations do not distinguish what type of wind (MHD vs photoevaporative) nor they cannot distinguish different types of photoevaporative flows (red line: EUV driven while blue line: X-ray driven, Alexander 2008 and Ercolano & Owen 2010).

However, *line profiles alone cannot completely exclude an MHD wind*, see middle sketch of Figure 1 for an example of close-in MHD wind and discussion on the ambiguity of line profiles in Weber et al. (2020). Furthermore, *profiles alone cannot discriminate between different types of photoevaporative flows* as illustrated in Figure 2. Because both the EUV-driven (red line, Alexander 2008) and the X-ray-driven (blue line, Ercolano & Owen 2010) predict approximately the same density of Ne^+ ions, even though the bulk gas density differs by a factor $\sim$ 100, these models imply wind mass loss rates that differ by two orders of magnitude! However, an EUV-driven wind is completely ionized while an X-ray-driven wind is mostly neutral (ionization fractions of $\sim 0.1 - 0.01$), e.g. Owen et al. (2012). *Mapping photoevaporative winds in multiple forbidden and H I recombination lines, as proposed here, can discriminate between these two models and help quantify mass loss rates.*

Section 3 **The JWST/MIRI opportunity and our transition disk sample.** *As Spitzer/IRS was instrumental to discover a diagnostic tracing disk winds, so the sensitivity and spatial resolution of MIRI MRS can uniquely map the distribution of the Ne^+ emission, and other likely wind tracers, breaking degeneracies in line profile modeling and revealing the origin and magnitude of wind mass loss.*

The sensitivity and spatial resolution of ALMA has recently enabled us to resolve the inner regions of systems suspected to have large dust gaps or cavities based on their spectral energy distributions (e.g., Francis & van der Marel 2020). At the same time, a new study re-analyzing older and newer ground-based VISIR spectra ($R \sim 30,000$) has expanded the sample of disks with [Ne II] winds (Pascucci et al. 2020). From the overlapping sample of transition disks in Francis & van der Marel and wind sources in Pascucci et al., we select just two nearby ($\leq$100 pc) and isolated systems, T Cha and V4046 Sgr, for this pathfinder project. Both systems have a large mm dust cavity with radius $>$ 30 au and a compact inner mm emission extending to $\leq$ 4 au from the central star (Hendler et al. 2018, Francis & van der Marel 2020, and Figure 3). Because their spectrally resolved [Ne II] 12.8 μm profiles have small blueshifts[1], the ionized wind component is either flowing within 4 au or beyond $\sim$ 30 au. Finally, as shown in the lower panel of Figure 3, the [Ne II] is easily detected even in medium-resolution *Spitzer*/IRS spectra ($R \sim 700$) while the [Ne III] at 15.55 μm, which is expected to be an order of magnitude fainter (e.g., Hollenbach & Gorti 2009), is marginally detected (Lebouteiller et al. 2015, Rapson et al. 2015). The higher spectral resolution of MIRI MRS will boost the line-to-continuum ratio.

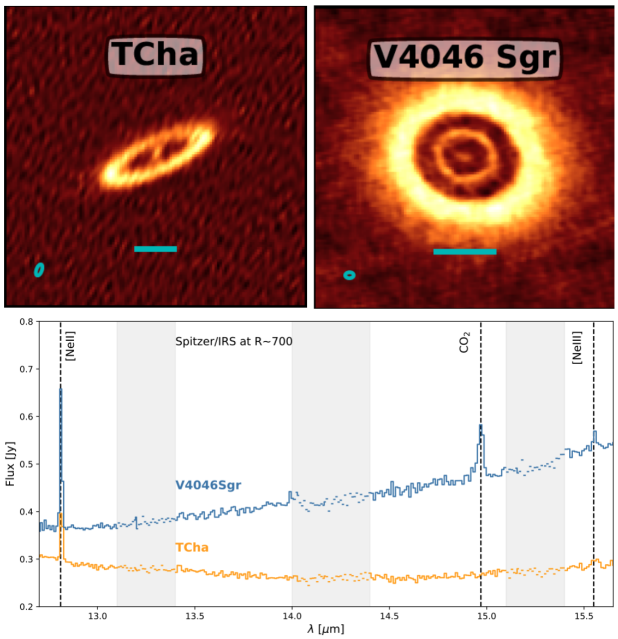

Figure 3: Top: Millimeter ALMA images of the T Cha and V4046 Sgr disks selected for this proposal (Francis & van der Marel 2020). The beam size is shown in the bottom left, the scalebar at the bottom is 30 au in length. The mm dust cavities in T Cha and V4046 Sgr are 68 au (0.6″) and 62 au (0.8″) in diameter, respectively and can be resolved with JWST/MIRI. Bottom: Medium-resolution *Spitzer*/IRS spectra showing the strong [Ne II] and tentative [Ne III] detections (CASSIS database, Lebouteiller et al. 2015). As MIRI MRS has a spectral resolution $\sim$ 3 times higher than IRS and [Ne II] FWHMs are only $\sim$ 30 km/s, the line-to-continuum ratio in MIRI spectra will be higher. Regions in grey lack data.

Section 4 **Pinning down a photoevaporative wind origin and mass loss rates.** Line profiles and line widths lead us to expect [Ne II] emission to originate near or exterior to the cavity radius ($>$ 30 au), in which case it will be resolved by JWST/MIRI MRS (see **Technical Justification**). Unresolved [Ne II] emission would unambiguously rule out a photoevaporative origin since a flow within 4 au is so deep in the gravitational potential well of these stars that cannot be thermally driven. Additionally, the spatial distribution of [Ne II] emission at

[1]Shocked gas in jets is excluded in these systems since jets have larger blueshifts (>30 km/s) and FWHMs ($\sim$ 50 km/s) and are also easily detected in the [O I] 6300 Å (Pascucci et al. 2020).

12.81 μm will break degeneracies in line modeling. In a high density X-ray-driven photoevaporative wind, [Ne II] emission is limited by the penetration depth of ionizing photons and it is shown to be restricted to a thin skin tracing the flow from the rim of a large cavity (e.g., Ercolano & Owen 2020 and Picogna et al 2019). In contrast, low density EUV-driven winds (e.g., Alexander 2008) are optically thin to the photons that ionize neon and the emission is correspondingly more radially extended (e.g., Ballabio et al. 2020). [Ne II]/[Ne III] and [Ne II]/[Ar II] ratios also help in discriminating between soft/hard X-rays and EUV photons heating and ionizing the flow (e.g., Hollenbach & Gorti 2009, Szulágyi et al. 2012, Espaillat et al. 2013). In addition, both EUV and X-ray driven flows are partly ionized and will show H I recombination emission which is temperature sensitive and will not be co-spatial with [Ne II] emission for X-ray ionized gas (e.g., Ercolano & Owen 2010). Finally, cold radially extended MHD winds (e.g., Bai 2016) would also show extended [Ne II] emission beyond the cavity radius but can be distinguished from EUV-driven photoevaporative winds because, being little ionized, they would not show H I recombination line emission near or exterior to the cavity radius. Although the luminosity of the spectrally and spatially unresolved H I lines detected by *Spitzer* points to most of the emission tracing accretion of disk gas onto the star (e.g., Rigliaco et al. 2015), our deep observations with MIRI MRS can detect and resolve the fainter wind component at the cavity radius (see **Technical Justification**).

Science objectives. Our primary objective is to spatially resolve the [Ne II] 12.81 μm emission from the two transition disks shown in Figure 3 with MIRI/MRS IFU. As their blueshifted [Ne II] profiles confine the ionized flow either within 4 au or beyond 30 au, the extent of the [Ne II] emission obtained with MIRI will pin down the origin of the wind: closer-in MHD (unresolved emission) vs. X-ray-driven photoevaporative (narrow ring at the cavity radius) vs. EUV-driven photoevaporative or cold MHD wind (extended emission beyond the cavity radius). Our secondary objective is to map the wind in other forbidden lines and in the strongest of the H I recombination lines. Although these lines are fainter than the [Ne II] at 12.81 μm, they uniquely constrain the shape of the radiation field impinging on the disk and can discriminate between an ionized low density EUV-driven flow and a cold radially extended MHD wind. The combination of these tracers will quantify the ionization fraction of the flow and determine whether these systems are driving a low density (mass loss rate $\sim 10^{-10}$ M$_\odot$/yr) or a high density flow (mass loss rate $\sim 10^{-8}$ M$_\odot$/yr). Additionally, forward modeling using the density fields for EUV and X-ray photoevaporative winds (e.g., Alexander 2008, Clarke & Alexander 2016, Picogna et al. 2019) or MHD similarity solutions (Lesur 2020), combined with radiative transfer calculations, can further refine wind mass loss rates. Thus, regardless of whether the dust cavity is opened by photoevaporation or by one or more giant planets, constraining wind mass loss rates will inform us on how much time is left before the gaseous disk disperses. This, in turn, will set the time available for further planet formation and migration.

Section 5